

# Resonant magneto-conductance of a suspended carbon nanotube quantum dot

G. RASTELLI<sup>1(a)</sup>, M. HOUZET<sup>2</sup> and F. PISTOLESI<sup>3,1</sup>

<sup>1</sup> *Laboratoire de Physique et Modélisation des Milieux Condensés, Université Joseph Fourier and CNRS F-38042 Grenoble, France, EU*

<sup>2</sup> *CEA, INAC, SPSMS - F-38054 Grenoble, France, EU*

<sup>3</sup> *Centre de Physique Moléculaire Optique et Hertzienne, Université de Bordeaux I and CNRS F-33405 Talence, France, EU*

received 14 December 2009; accepted in final form 17 February 2010  
published online 19 March 2010

PACS 73.63.-b – Electronic transport in nanoscale materials and structures

PACS 71.38.-k – Polarons and electron-phonon interactions

PACS 85.85.+j – Micro- and nano-electromechanical systems (MEMS/NEMS) and devices

**Abstract** – We address the electronic resonant transport in the presence of a transverse magnetic field through the single level of a suspended carbon nanotube acting as a quantum oscillator. We predict a negative magneto-conductance with a magnetic-field-induced narrowing of the resonance line and a reduction of the conductance peak when the nanotube is asymmetrically contacted to the leads. At finite bias voltage we study the threshold for phonon-assisted transport.

Copyright © EPLA, 2010

**Introduction.** – A distinctive non-classical feature of any quantum state is the possibility that part of the system is spatially delocalized. Probing delocalization in macroscopic systems is important to validate quantum mechanics on that scale [1]. For large molecules, this has been done by the observation of interference fringes with diffraction experiments [2]. Is it possible to observe quantum delocalization for a mechanical oscillator? Nano-electromechanical systems are bridging the gap between the microscopic and macroscopic length scale and they offer a unique opportunity to answer this question [3–11]. A particularly promising system is the suspended carbon nanotube [12,13]. It has been recently predicted that the magneto-conductance can be used as a detector of the quantum delocalization of a suspended carbon nanotube due to the Aharonov-Bohm effect on the electrons crossing the device [14] (see fig. 1 for a schematic representation of the system).

A qualitative picture of the effect is the following: the carbon nanotube's mechanical ground state is a quantum superposition of displaced oscillator states. When an electron crosses the device, its wave function acquires an Aharonov-Bohm phase that depends on the position of the displaced oscillator. The total transmission results from the interference of all electronic trajectories. Thus

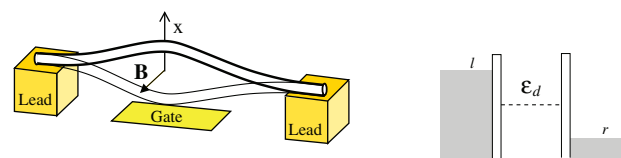


Fig. 1: (Colour on-line) Left: schematic picture of the system: a voltage biased suspended carbon nanotube in the presence of a transverse magnetic field  $B$ . Right: positions of the electronic levels for the resonant transport.

the Aharonov-Bohm phases generate a magnetic-field dependence of the current that would be absent in the case of a *single* classical path. This spectacular prediction was done in the tunnel regime. Though simple and transparent from the technical point of view, this regime is not optimal for the experimental observation of the effect for two reasons: i) the current is very low, ii) electrons can interfere only once since a single crossing through the device contributes to the current.

In this article, we consider the resonant transport through a single-electron state of the nanotube quantum dot. At resonance, the electron channel is fully open for a static nanotube. One could expect that the magneto-conductance signal for the suspended nanotube will be greatly enhanced: the electrons bounce many times inside the structure before leaving, therefore allowing multiple

<sup>(a)</sup>E-mail: gianluca.rastelli@grenoble.cnrs.fr

interference. Thus, even if the phase acquired at each passage is small, the accumulated phase can be large. By performing a calculation with Keldysh non-equilibrium Green's function technique at lowest order in the electron-phonon coupling, we find the following results: the shape of the resonance as a function of the gate voltage is modified by the magnetic field. Far from the resonance, the tunneling magneto-conductance of ref. [14] is recovered. At resonance and for vanishing temperature, the linear conductance depends on the magnetic field only if the coupling to the leads is asymmetric, while the resonance width is reduced by the magnetic field. The current-voltage characteristics shows a magnetic-field-dependent singularity at the threshold of one-phonon absorption. These prominent features constitute a measurable signature of the quantum delocalization of the nanotube.

**Model Hamiltonian.** – We model the system with the following Hamiltonian:

$$H = \sum_{\nu=l,r} \sum_k \xi_{k\nu} a_{k\nu}^\dagger a_{k\nu} + \varepsilon_d a_d^\dagger a_d + \hbar\omega b^\dagger b + H_T. \quad (1)$$

Here,  $a_{kl}^\dagger$  ( $a_{kr}^\dagger$ ) is a creation operator for the electronic single-particle states in the left (right) lead. The energy spectrum in each lead is  $\xi_{k\nu} = \varepsilon_k - \mu_\nu$ , where the difference of the chemical potentials  $\mu_r - \mu_l = eV$  is related to the bias voltage  $V$ . The leads are connected by a suspended nanotube placed in a strong magnetic field perpendicular to the nanotube's oscillation plane (see fig. 1). We single out the fundamental bending mode with resonance frequency  $\omega$  for which  $b^\dagger$  is the creation operator of quantum excitations. The single relevant electronic level in the nanotube for which  $a_d^\dagger$  is a creation operator sits at energy  $\varepsilon_d$  that can be controlled with an external gate voltage. For simplicity, we consider fully spin-polarized electrons (having in mind the large magnetic field for which our theory applies) and neglect a possible orbital degeneracy in the nanotube. The last term in eq. (1) models electron transfer from the leads to the nanotube in the presence of the magnetic field [14]:

$$H_T = \sum_{\nu=l,r} \sum_k t_\nu e^{i\phi_\nu x} a_{k\nu}^\dagger a_d + \text{h.c.}, \quad (2)$$

where  $t_l$  and  $t_r$  are the tunneling matrix elements at the point contacts between the nanotube and the leads. The magnetic field  $B$  enters the Hamiltonian through Aharonov-Bohm phases  $\phi_\nu x$  that depend on the quantum displacement of the nanotube (a global diamagnetic energy shift is absorbed into  $\varepsilon_d$ ) [14]. Here,  $x = b + b^\dagger$  is the displacement operator of the nanotube's bending mode in units of the amplitude  $u_0$  for zero-point fluctuations. The factor  $\phi \equiv \phi_l = -\phi_r = gBLu_0/\Phi_0$  is the magnetic flux (in units of the flux quantum  $\Phi_0 = h/e$ ) through the area swept by the nanotube of length  $L$  in the ground-state quantum fluctuation ( $g$  is a geometrical factor of order one related to the deflection of the bending mode).

In absence of magnetic field ( $\phi=0$ ) the system is non-interacting and the Hamiltonian (1) can be studied exactly: it describes the resonant transport through a single electronic level as well as a decoupled oscillator mode. The parameter  $\phi$  is thus the electron-phonon coupling constant of the problem. In the Discussion section, we will argue that  $\phi$  is typically very small in realistic systems. We thus perform a perturbative calculation in  $\phi$  ( $\propto B$ ) around the non-interacting solution. This method provides the exact expansion in  $B$  of the current:

$$I(B) = I(0) + \frac{B^2}{2} \left. \frac{d^2 I}{dB^2} \right|_{B=0} + \dots, \quad (3)$$

without any further approximation (the result is at all orders in  $t_\nu$ ). In particular, the expressions derived below also apply when the gate voltage is tuned near a resonance. In contrast, those of ref. [14] are based on a perturbative expansion in the tunneling matrix elements; therefore they only hold in the off-resonant regime.

We note that the Hamiltonian (1) resembles the one proposed to study polaronic transport through a vibrating molecule [15,16] (there  $\phi_l = \phi_r$ ,  $\varepsilon_d$  includes a polaronic shift  $-\phi^2\omega$ , and  $x$  stands for dimensionless momentum), but they lead to qualitative different behavior. The Hamiltonian of ref. [17] describing Coulomb blockade at resonant tunneling reduces to (1) for a single-mode electromagnetic environment associated with the fluctuations of the bias voltage. In this case, the effect of the environment on the conductance was only addressed at large bias voltage or far from the resonance.

**Keldysh Green's functions approach.** – The current operator in the left lead is  $\hat{I} \equiv (ie/\hbar)[H, N_l]$ , with  $N_l = \sum_k a_{kl}^\dagger a_{kl}$ . In the stationary regime, the dc current flowing through the device is

$$I = -\frac{ie}{\hbar} \sum_k \left( t_l \langle e^{i\phi x} a_{kl}^\dagger a_d \rangle - \text{c.c.} \right), \quad (4)$$

where the brackets denote a quantum-statistical average. In order to evaluate the current, we use Keldysh theory for non-equilibrium systems [18]. We define the retarded, advanced, and Keldysh electronic Green's functions:

$$G_{n,n'}^{R/A}(t) = \mp i \theta(\pm t) \langle \{ a_n(t), a_{n'}^\dagger(0) \} \rangle, \quad (5)$$

$$G_{n,n'}^K(t) = -i \langle [ a_n(t), a_{n'}^\dagger(0) ] \rangle, \quad (6)$$

(with  $n, n' = kl, k'r, d$ ) and we define the matrix

$$\hat{G} = \begin{pmatrix} G^R & G^K \\ 0 & G^A \end{pmatrix}. \quad (7)$$

We define similarly a Green's function  $\hat{G}_{xd,kl}$  related to eq. (4), such that, for instance,

$$G_{xd,kl}^{R/A}(t) = \mp i \theta(\pm t) \langle \{ a_d(t) e^{i\phi x(t)}, a_{kl}^\dagger(0) \} \rangle. \quad (8)$$

The relation

$$\hat{G}_{kl,k'l}(\varepsilon) = \hat{g}_{kl}(\varepsilon)\delta_{k,k'} + \hat{g}_{kl}(\varepsilon)t_l\hat{G}_{xd,k'l}(\varepsilon) \quad (9)$$

holds in Fourier space, where  $\hat{g}_{kl}$  is the Green's function in the uncoupled left lead (at  $H_T = 0$ ). We introduce  $\hat{g}_\nu = \sum_k \hat{g}_{k\nu}$  and  $\hat{G}_{\nu,\nu'} = \sum_{k,k'} \hat{G}_{k\nu,k'\nu'}$ . In the wide-band limit:  $g_\nu^{R/A} = \mp i\pi\rho_\nu$ ,  $g_\nu^K = 2[1 - 2n_\nu]g_\nu^R$ , where  $\rho_\nu$  are the densities of states in the leads and  $n_\nu(\varepsilon) = n_F(\varepsilon - \mu_\nu)$ , with  $n_F$  the Fermi distribution function at temperature  $T$ . Then, eq. (4) can be rewritten as

$$I = -\frac{e}{h}\text{Re} \int d\varepsilon \left[ \hat{g}_l^{-1}(\varepsilon)\hat{G}_{l,l}(\varepsilon) \right]_{12}. \quad (10)$$

*Non-interacting theory.* In the absence of magnetic field the electron-phonon coupling ( $\phi = 0$ ) vanishes, the Green's function on the dot is known:

$$G_{d,d}^{(0)R/A}(\varepsilon) = (\varepsilon - \varepsilon_d \pm i\Gamma)^{-1}, \quad (11)$$

$$G_{d,d}^{(0)K}(\varepsilon) = -2i \sum_{\nu=l,r} \frac{\Gamma_\nu[1 - 2n_\nu(\varepsilon)]}{(\varepsilon - \varepsilon_d)^2 + \Gamma^2}. \quad (12)$$

Here,  $\Gamma = \Gamma_l + \Gamma_r$  and  $\Gamma_\nu = \pi\rho_\nu|t_\nu|^2$  give the broadening of the resonant level due to its hybridization with the leads. Then, one gets

$$\hat{G}_{l,l}^{(0)} = \hat{g}_l + \hat{g}_l t_l \hat{G}_{d,d}^{(0)} t_l^* \hat{g}_l. \quad (13)$$

Inserting this into eq. (10), one retrieves the result

$$I^{(0)} = (e/h) \int d\varepsilon [n_l(\varepsilon) - n_r(\varepsilon)] \mathcal{T}(\varepsilon), \quad (14)$$

with the elastic Breit-Wigner transmission coefficient through the non-interacting resonant level

$$\mathcal{T}(\varepsilon) = 4\Gamma_l\Gamma_r/[(\varepsilon - \varepsilon_d)^2 + \Gamma^2]. \quad (15)$$

In particular, the linear conductance at resonance and  $T = 0$ ,  $G_{\text{max}} = (e^2/h)4\Gamma_l\Gamma_r/\Gamma^2$ , reaches the conductance quantum for symmetric contacts ( $\Gamma_l = \Gamma_r$ ).

*Second-order perturbation theory.* We now consider the coupling with phonons perturbatively. To lowest order in  $\phi$ , the Green's functions read

$$\hat{G}_{l,l}(\varepsilon) = \hat{G}_{l,l}^{(0)}(\varepsilon) + \sum_{n,n'=l,r,d} \hat{G}_{l,n}^{(0)}(\varepsilon)\hat{\Sigma}_{n,n'}^{(2)}(\varepsilon)\hat{G}_{n',l}^{(0)}(\varepsilon). \quad (16)$$

The self-energies  $\hat{\Sigma}_{n,n'}^{(2)}$  are represented schematically in fig. 2 by one-loop diagrams. The first diagram arises from the terms proportional to  $\phi^2 x^2$  in the perturbative expansion of eq. (2) with respect to  $\phi$ . It leads to a renormalization of tunneling matrix elements:  $t_\nu \rightarrow t_\nu(1 - \phi^2 \langle x^2 \rangle_0/2)$ , where  $\langle x^2 \rangle_0 = \coth[\hbar\omega/(2k_B T)]$  for the unperturbed oscillator. The second diagram accounts for the shift of the oscillator's position,  $\langle x \rangle_\phi = 4\phi I^{(0)}/(e\omega)$ . This shift can be interpreted classically; it is the equilibrium shift resulting from the interplay between the elastic force and the force

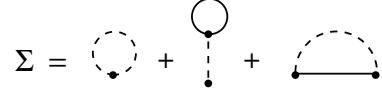


Fig. 2: Diagrams for the self-energy. Dots denote vertices for tunneling from the single level to the leads, full and dashed lines stand for electron and phonon Green's functions, respectively.

$\propto -\langle \partial H_T / \partial x \rangle$  that scales linearly with the magnetic field and the current flowing through the structure (similar to the Laplace force on a current-carrying wire). It does not contribute to the current to order  $\phi^2$ . The third diagram contains the non-trivial part of the electron-phonon interaction. The sum of the three diagrams reads

$$\hat{\Sigma}_{n,n'}^{(2)} = \tilde{t}_{nn'} + \sum_{m,m'=l,r,d} A_{nn'}^{mm'} \hat{\sigma}_{m,m'}, \quad (17)$$

where  $\tilde{t}_{l,d} = \tilde{t}_{d,l}^* = t_l(i\phi \langle x \rangle_\phi - \phi^2 \langle x^2 \rangle_0/2)$ ,  $\tilde{t}_{r,d} = \tilde{t}_{d,r}^* = t_r(-i\phi \langle x \rangle_\phi - \phi^2 \langle x^2 \rangle_0/2)$ ,  $A_{\nu\nu'}^{dd} = A_{dd}^{\nu\nu'*} = \phi_\nu \phi_{\nu'} t_\nu t_{\nu'}^*$ ,  $A_{\nu d}^{d\nu'} = A_{d\nu'}^{d\nu*} = -\phi_\nu \phi_{\nu'} t_\nu t_{\nu'}^*$  ( $\nu, \nu' = l, r$ ) and zero otherwise. The components of  $\hat{\sigma}_{n,n'}$  ( $n, n' = l, r, d$ ) read

$$\begin{aligned} \sigma_{n,n'}^{R/A}(t) &= \frac{i}{2} \left[ G_{n,n'}^{(0)R/A}(t) D^K(t) + G_{n,n'}^{(0)K}(t) D^{R/A}(t) \right], \\ \sigma_{n,n'}^K(t) &= \frac{i}{2} \left[ G_{n,n'}^{(0)R}(t) D^R(t) + G_{n,n'}^{(0)A}(t) D^A(t) \right. \\ &\quad \left. + G_{n,n'}^{(0)K}(t) D^K(t) \right]. \end{aligned} \quad (18)$$

Here,  $\hat{D}$  is the Green's function for unperturbed phonons (at  $\phi = 0$ ):

$$\begin{aligned} D^{R/A}(\varepsilon) &= 2\hbar\omega/[(\varepsilon \pm i0^+)^2 - (\hbar\omega)^2], \\ D^K(\varepsilon) &= -2i\pi[\delta(\varepsilon - \hbar\omega) + \delta(\varepsilon + \hbar\omega)] \coth \left[ \frac{\hbar\omega}{2k_B T} \right]. \end{aligned}$$

**Results.** – Evaluation of the current up to  $\phi^2$  terms by inserting eqs. (16)–(18) into (10) is now straightforward. After extended calculations, we get  $I = I^{(0)} + \phi^2 I^{(2)} + \dots$ , where

$$\begin{aligned} I^{(2)} &= \frac{G_{\text{max}}}{e} \left[ \int d\varepsilon [n_l(\varepsilon) - n_r(\varepsilon)] \mathcal{T}^a(\varepsilon) \right. \\ &\quad \left. + \sum_{\nu,\nu'=l,r} \left( \int d\varepsilon [1 - n_{\nu'}(\varepsilon - \hbar\omega)] n_\nu(\varepsilon) \mathcal{T}_{\nu,\nu'}^b(\varepsilon) \right. \right. \\ &\quad \left. \left. + \int \int d\varepsilon d\varepsilon' [1 - n_{\nu'}(\varepsilon')] n_\nu(\varepsilon) \mathcal{T}_{\nu,\nu'}^c(\varepsilon, \varepsilon') \right) \right]. \end{aligned} \quad (19)$$

The coefficients

see eqs. (20) on the next page

are expressed through the functions  $a(\varepsilon) = \text{Re}[\Gamma G_{d,d}^A(\varepsilon)]$ ,  $b(\varepsilon) = \text{Im}[\Gamma G_{d,d}^A(\varepsilon)]$ ,  $c(\varepsilon, \varepsilon') = a(\varepsilon)a(\varepsilon') + b(\varepsilon)b(\varepsilon')$ , and  $d(\varepsilon, \varepsilon') = a(\varepsilon)b(\varepsilon') - b(\varepsilon)a(\varepsilon')$ , while  $s_l = 1$ ,  $s_r = -1$ ,  $\gamma = (\Gamma_L - \Gamma_R)/\Gamma$  is an asymmetry factor for the coupling

$$\mathcal{T}^a(\varepsilon) = -2a(\varepsilon)[a(\varepsilon + \hbar\omega) + a(\varepsilon)] - 4\gamma^2 b(\varepsilon)c(\varepsilon, \varepsilon + \hbar\omega) - [2b(\varepsilon) - b(\varepsilon + \hbar\omega) - b(\varepsilon - \hbar\omega)]n_B, \quad (20a)$$

$$\begin{aligned} \mathcal{T}_{\nu,\nu'}^b(\varepsilon) = & s_\nu(1 - \delta_{\nu,\nu'})[a(\varepsilon) + a(\varepsilon - \hbar\omega)]^2 + 2s_\nu(\delta_{\nu,\nu'}(1 - 2\gamma^2) + \gamma^2)c(\varepsilon, \varepsilon - \hbar\omega)[b(\varepsilon - \hbar\omega) + (1 - 2\delta_{\nu,\nu'})b(\varepsilon)] \\ & + (2\delta_{\nu,\nu'} - 1)b(\varepsilon)b(\varepsilon - \hbar\omega)[b(\varepsilon - \hbar\omega) - b(\varepsilon)](\hbar\omega)^2(s_\nu\Gamma_\nu + s_{\nu'}\Gamma_{\nu'})/\Gamma^3, \end{aligned} \quad (20b)$$

$$\mathcal{T}_{\nu,\nu'}^c(\varepsilon, \varepsilon') = \frac{4}{\pi\Gamma} \frac{s_\nu\Gamma_\nu\hbar\omega}{(\hbar\omega)^2 - (\varepsilon - \varepsilon')^2} \{a(\varepsilon)[b(\varepsilon) + b(\varepsilon')] + 2s_{\nu'}\gamma b(\varepsilon)d(\varepsilon, \varepsilon')\}, \quad (20c)$$

to the contacts, and  $n_B = [e^{\hbar\omega/k_B T} - 1]^{-1}$  is the Bose factor. The two first terms in the r.h.s. of eq. (19) express elastic as well as inelastic electron tunneling with emission/absorption of one phonon. The last term cannot be interpreted as a single-particle elementary process: it is related to the many-body character of the Fermi sea in the leads [17,19,20]. In the following, we discuss the result for the current in several regimes.

*Vanishing bias regime.* Let us start with considering the linear conductance  $G \equiv (dI/dV)_{V=0} = G^{(0)} + \phi^2 G^{(2)} + \dots$ . At zero temperature, we obtain  $G^{(2)}$  from eq. (19):

$$\begin{aligned} G^{(2)} = & -G_{\max} \sum_{s=\pm} \left\{ -\frac{sB_s(\mu)}{\pi} \ln \left( \frac{\hbar^2\omega^2}{\Gamma^2 + \tilde{\varepsilon}_d^2} \right) \right. \\ & \left. + A_s(\mu) \left[ 1 - \frac{2s}{\pi} \arctan \left( \frac{\tilde{\varepsilon}_d}{\Gamma} \right) \right] + a^2(\mu) \right\}, \end{aligned} \quad (21)$$

where  $\tilde{\varepsilon}_d = \varepsilon_d - \mu$  ( $\mu = \mu_l = \mu_r$ ),  $A_\pm(\mu) = a(\mu)a(\mu \pm \hbar\omega) + 2\gamma^2 b(\mu)c(\mu, \mu \pm \hbar\omega)$  and  $B_\pm(\mu) = a(\mu)b(\mu \pm \hbar\omega) + 2\gamma^2 b(\mu)d(\mu, \mu \pm \hbar\omega)$ . As  $G^{(2)} < 0$ , the magneto-conductance  $\Delta G = G - G^{(0)}$  is always negative. Its gate-voltage dependence is illustrated numerically for different parameters of the junction in fig. 3. The negative sign of  $G^{(2)}$  results in a narrowing of the resonance line at finite magnetic field. This is shown numerically in fig. 4. As in the polaronic transport problem [20], there is no vibrational sideband at  $\tilde{\varepsilon}_d = \pm\hbar\omega$  in the gate-voltage dependence of the linear conductance. Such sidebands only appear at finite bias voltage due to inelastic transitions (see below).

Let us now consider the conductance peak at resonance. It is obtained from eq. (21) at  $\tilde{\varepsilon}_d = 0$ :

$$G_{\text{res}}^{(2)} = -G_{\max} \frac{4\gamma^2\Gamma^2}{\Gamma^2 + (\hbar\omega)^2} \left[ 1 + \frac{2\hbar\omega}{\pi\Gamma} \ln \left( \frac{\hbar\omega}{\Gamma} \right) \right]. \quad (22)$$

Remarkably  $G_{\text{res}}^{(2)}$  vanishes only at symmetric coupling between the dot and the leads ( $\gamma=0$ ). This feature explains the qualitative difference between left and right panels in figs. 3 or 4. This is in contrast with the polaronic model where  $G_{\text{res}}^{(2)} = 0$  at any  $\gamma$  [17]. The last identity can be attributed to the symmetric role played by the left and right leads at  $V=0$  in the polaronic case ( $\phi_l = \phi_r$ ), while such a symmetry does not exist in our model.

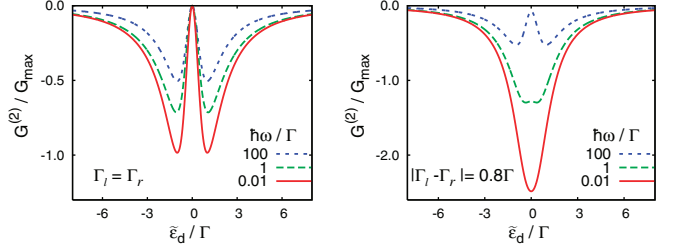


Fig. 3: (Colour on-line) Gate-voltage dependence of the magneto-conductance at  $T=0$  and different values of  $\hbar\omega/\Gamma$ , for a nanotube contacted symmetrically (left) or asymmetrically (right) to the leads.

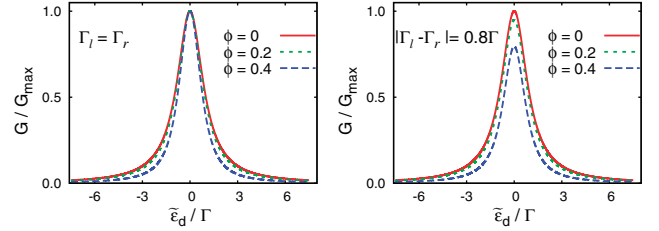


Fig. 4: (Colour on-line) Gate-voltage dependence of the conductance at  $T=0$ , for different values of the magnetic field ( $\phi = 0, 0.2, 0.4$ ) and  $\hbar\omega = \Gamma$ , for a nanotube contacted symmetrically (left) or asymmetrically (right) to the leads.

Another feature seen in fig. 3 is that the magneto-conductance is more pronounced at small resonance frequency. Actually, simple expressions can be obtained from eq. (21) in the adiabatic regime ( $y \equiv \hbar\omega/\Gamma \ll 1$ ):

$$G_{\text{ad}}^{(2)} = -4G_{\max}\Gamma^2[\tilde{\varepsilon}_d^2 + \gamma^2\Gamma^2]/[\tilde{\varepsilon}_d^2 + \Gamma^2]^2, \quad (23)$$

and in the anti-adiabatic regime ( $y \gg 1$ ):

$$G_{\text{non-ad}}^{(2)} = -2G_{\max}\tilde{\varepsilon}_d^2\Gamma^2/[\tilde{\varepsilon}_d^2 + \Gamma^2]^2. \quad (24)$$

Note that  $G_{\text{ad}}^{(2)} = 2G_{\text{non-ad}}^{(2)}$  for a symmetric junction. While we don't have an explanation for eq. (23), the anti-adiabatic result (24) receives a simple interpretation [17]: at high resonance frequency, the harmonic oscillator remains in its ground state,  $|0\rangle$ , and an effective Hamiltonian for electron tunneling in the device is obtained by projecting eq. (1) on this state. This describes a non-interacting resonant level coupled to the leads through renormalized tunneling matrix elements  $t_\nu \langle 0|e^{i\phi_\nu x}|0\rangle = t_\nu e^{-\phi^2/2}$  with corresponding level widths



$\Gamma_\nu e^{-\phi^2}$ . As a result, the resonance narrows, but the maximum transmission is unchanged. Equation (24) expresses this in lowest order in the coupling constant. Actually, the conductance reduction in asymmetric junctions arises to higher order in the expansion in  $1/y \ll 1$ :  $\Delta G_{\text{res}}/G_{\text{max}} \propto -\phi^2 \gamma^2 (\ln y)/y$ .

Is the magnetic-field-induced correction to the current really due to the quantum vibrations of the oscillator? To answer this question, we first consider the magneto-conductance at temperature  $k_B T \gg \hbar\omega$  and we find from eq. (19) that it is suppressed like

$$\frac{\Delta G(T)}{G^{(0)}(T)} = -\phi^2 \frac{\hbar\omega}{k_B T} \times \begin{cases} \frac{4}{3} \frac{\tilde{\varepsilon}_d^2 + \gamma^2 \Gamma^2}{\tilde{\varepsilon}_d^2 + \Gamma^2}, & k_B T \ll \Gamma, \\ \frac{1}{2 \cosh^2(\tilde{\varepsilon}_d/2k_B T)}, & k_B T \gg \Gamma. \end{cases} \quad (25)$$

Thus, the answer seems positive. Surprisingly to us however, a temperature dependence  $\Delta G(T)/G^{(0)}(T) \propto -\phi^2 \hbar\omega/k_B T$  may also arise classically as we now explain. Indeed, in the classical case, the electronic part of the Hamiltonian (1) still holds, while the displacement  $x$  entering (2) is a time-varying classical field that obeys an oscillator's equation of motion in the presence of a Langevin force describing thermal fluctuations. Formally,  $x(t)$  acts as an external bias voltage  $V_{\text{ac}} = 2\phi(\hbar/e)\dot{x}(t)$  in eq. (2). The current  $I(t)$  through a resonant level can then be calculated at arbitrary bias voltage  $V + V_{\text{ac}}(t)$  following ref. [21]. The dc component of  $I(t)$  is then obtained after averaging over the thermal fluctuations. The result coincides with the term proportional to  $n_B$  in the formula (19)–(20). When  $k_B T \gg \hbar\omega$  one finds

$$\frac{\Delta G_{\text{cl}}(T)}{G^{(0)}(T)} = -\phi^2 \frac{\hbar\omega}{k_B T} \times \begin{cases} \frac{2k_B^2 T^2 (\Gamma^2 - 3\tilde{\varepsilon}_d^2)}{(\tilde{\varepsilon}_d^2 + \Gamma^2)^2}, & k_B T \ll \Gamma, \\ \frac{1 - 3\text{th}^2(\tilde{\varepsilon}_d/2k_B T)}{2}, & k_B T \gg \Gamma. \end{cases} \quad (26)$$

Thus the quantum and classical results, eqs. (25) and (26) respectively, do not coincide. Overall, the quantum fluctuation of the mechanical oscillator is necessary to account for the magneto-conductance studied in this work. It cannot be interpreted as a classical rectification effect of the thermal fluctuation in the oscillator's position.

*Finite bias regime.* The formula (19) for the current also allows to address the finite bias non-linear regime. The possibility to excite the phonon (inelastic cotunneling) when  $eV > \hbar\omega$  leads to a non-analytical voltage dependence of the current in vicinity of the threshold at  $T = 0$ , with leading terms:

$$\frac{1}{G_{\text{max}}} \frac{dI^{(2)}}{dV} = \frac{c_1}{2\pi} \ln \frac{\Gamma}{|eV - \hbar\omega|} + 4c_2 \theta(eV - \hbar\omega), \quad (27)$$

and asymptotic expressions for the coefficients

$$c_1 = \begin{cases} -8\hbar\omega\Gamma^3 (\gamma^2\Gamma^2 + \tilde{\varepsilon}_d^2) / (\Gamma^2 + \tilde{\varepsilon}_d^2)^3, & \hbar\omega \ll \Gamma, \\ -\gamma(4\Gamma/\hbar\omega)^4 \tilde{\varepsilon}_d/\Gamma, & \hbar\omega \gg \Gamma, \end{cases}$$

and

$$c_2 = \begin{cases} \Gamma^2(\gamma^2\Gamma^2 + \tilde{\varepsilon}_d^2) / (\Gamma^2 + \tilde{\varepsilon}_d^2)^2, & \hbar\omega \ll \Gamma, \\ (2\Gamma/\hbar\omega)^4 (\tilde{\varepsilon}_d^2 + \gamma^2\Gamma^2)/\Gamma^2, & \hbar\omega \gg \Gamma. \end{cases}$$

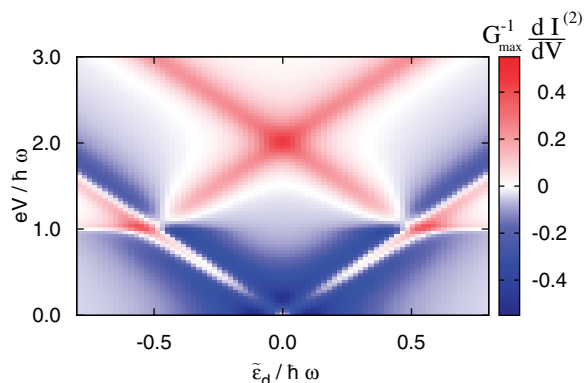


Fig. 5: (Colour on-line) Gate and bias voltage dependence of the differential conductance  $dI^{(2)}/dV$  at  $T=0$  for  $\hbar\omega = 10\Gamma$  and  $\Gamma_r = \Gamma_l$ .

A similar feature has been discussed for the polaron problem [22]. It is clearly seen in the gate and bias voltage dependence of the magneto-conductance shown in fig. 5. In addition, fig. 5 shows how the standard sequential tunneling lines at  $\tilde{\varepsilon}_d = \pm eV/2$  narrow at finite magnetic field, while additional phonon-assisted tunneling lines appear at  $\tilde{\varepsilon}_d = \pm(eV/2 - \hbar\omega)$ .

A weak electron-phonon coupling approximation up to the order  $\phi^2$  was used to obtain eq. (27). It overlooks several features that deserve further study. First, above the inelastic threshold ( $eV > \hbar\omega$ ), the phonon mode is driven out of equilibrium. By analogy with the polaron problem, we estimate that our results remain valid beyond the threshold in a region of voltage bias  $\delta V \equiv V - \hbar\omega/e \ll \hbar\omega/e$  [20] under the additional condition that the current-induced damping of the oscillator  $\sim \phi^2 \min[\hbar^2\omega^3/\Gamma^2, \Gamma/\hbar]$  remains much smaller than  $\omega$  [22]. Second, the non-linear electron-phonon coupling in the tunnel Hamiltonian (2) may lead to multi-phonon processes, while we only kept a linear electron-phonon coupling in leading order in  $\phi \ll 1$ . At larger  $\phi$ , we could thus expect that additional inelastic lines corresponding to multi-phonon absorption would appear at  $\tilde{\varepsilon}_d = \pm(eV/2 - n\hbar\omega)$  [23] and lead to a magnetic-field-induced current suppression similar to the electrostatic Franck-Condon blockade [24] recently observed experimentally [25].

*Tunnel regime.* The tunnel regime is realized at  $eV, k_B T, \hbar\omega \ll \Gamma \ll \tilde{\varepsilon}_d$ , far from the resonance and when the energy dependence of the transmission coefficient (15) can be neglected. In this limit, we find from eq. (21) that the magneto-conductance at  $T=0$  is negative:  $\Delta G_{\text{tun}} = -4\phi^2 G_{\text{tun}}^{(0)}$ , where  $G_{\text{tun}}^{(0)} = (4e^2/h)\Gamma_l\Gamma_r/\tilde{\varepsilon}_d^2$ , and from eq. (25) that it vanishes at high temperature like  $\Delta G_{\text{tun}}/G_{\text{tun}}^{(0)} = -4\phi^2 \hbar\omega/(3k_B T)$ , in agreement with ref. [14]. In contrast, the classical magneto-conductance vanishes exactly. Indeed, in the tunnel regime a linear current-voltage relation holds at any time:  $I(t) = G_{\text{tun}}^{(0)} [V + 2\phi(\hbar/e)\dot{x}(t)]$  and  $\Delta G_{\text{cl}} = 0$  since  $\langle \dot{x} \rangle_{\text{cl}}$  vanishes.

**Discussion.** – Let us now discuss the experimental conditions for the observation of the effect predicted in this article. The main difficulty is to reach a sufficiently large value of the coupling constant. For a single-wall nanotube of length  $L = 1 \mu\text{m}$ ,  $(\omega/2\pi) = 500 \text{ MHz}$ , one finds that the spatial amplitude for zero-point motion is  $u_0 \simeq 1 \text{ pm}$ . With  $B = 40 \text{ T}$ , one obtains a coupling constant  $\phi$  of the order of 0.1. This value is small, thus enabling the perturbative calculation presented above, but it is still large enough to lead to measurable effects. Actually, for  $\phi = 0.1$  the correction to the conductance can be of the order of few percents of the conductance quantum. Very recently, transport experiments through suspended carbon nanotubes have been performed [12,13] in a regime close to the one needed for the observation of the effects we describe. Similar experiment in a strong magnetic field of the order of 40 T should succeed in detecting the quantum delocalization by the Aharonov-Bohm effect.

Few comments are in order on the approximations leading to the Hamiltonian (1). It actually describes transport by reducing the carbon nanotube to a single electronic level coupled to the leads and by considering a single mechanical level. The fact that transport can be dominated by a single level in small quantum dots is well established experimentally; in particular, this has been observed in suspended carbon nanotubes [12,13,25]. The contribution of the other discrete mechanical modes deserves instead a short discussion. Each mode actually contributes to the magneto-conductance. But at the order  $B^2$  considered here, one can check that there is no interference between the different modes (interference would appear at order  $B^4$  due to the corrections to the phonon propagators). The  $B^2$  contribution to the current is thus simply given by the sum of the contributions of each mode according to eq. (19) with  $g$  and  $\omega$  factors related to the considered mode. In general one finds that the other mechanical modes contribute and slightly increase the intensity of the effect.

A different source of magnetic-field dependence of the current can be the shift of the electron levels induced by the modification of the electron wave function due to the Aharonov-Bohm interference through the loops of the atomic carbon structure (see, for instance, ref. [26]). It is unrelated to the presence of a phonon mode or to the quantum delocalization of the nanotube. In single-wall nanotubes, the typical magnetic-field scale is much larger than for the effect considered here. Moreover, the two origins for the magneto-conductance can be distinguished experimentally since they have totally different temperature and voltage dependence.

**Conclusion.** – We studied how the Aharonov-Bohm phase accumulated by the electrons crossing a vibrating nanotube affects its resonant magneto-conductance in the weak coupling regime. It was found that the shape of the conductance peak is modified by the coupling of the oscillator with the electronic transport induced by the

magnetic field. For realistic parameters the effect should be small, but still observable. We predict different temperature and voltage dependence of the magneto-current for a classical and a quantum oscillator. From the theoretical point of view, the Hamiltonian we studied is similar but not mappable to the polaron Hamiltonian describing charge transport through vibrating molecules. The strong coupling regime of the electron-phonon interaction constitutes a challenging and still open theoretical problem.

\*\*\*

We acknowledge important discussions with L. GLAZMAN. This work was supported by ANR through contract JCJC-036 NEMESIS.

## REFERENCES

- [1] LEGGETT A. J., *J. Phys: Condens. Matter*, **14** (2002) R415.
- [2] ARNDT M. *et al.*, *Nature*, **401** (1999) 680.
- [3] BLENCOWE M., *Phys. Rep.*, **395** (2004) 159.
- [4] LAHAYE M. D. *et al.*, *Science*, **304** (2004) 74.
- [5] SCHWAB K. C. and ROUKES M. L., *Phys. Today*, **58**, issue No. 7 (2005) 36.
- [6] NAIK A. *et al.*, *Nature*, **443** (2006) 193.
- [7] ARMOUR A. D. and BLENCOWE M. P., *New J. Phys.*, **10** (2008) 095004.
- [8] TEUFEL J. D., REGAL C. A. and LEHNERT K. W., *New J. Phys.*, **10** (2008) 095002.
- [9] PUGNETTI S., BLANTER Y. M. and FAZIO R., arXiv:0910.3900v1 (2009).
- [10] LAHAYE M. D. *et al.*, *Nature*, **459** (2009) 960.
- [11] ETAKI S. *et al.*, *Nat. Phys.*, **4** (2008) 785.
- [12] STEELE G. A. *et al.*, *Science*, **325** (2009) 1103.
- [13] LASSAGNE B. *et al.*, *Science*, **325** (2009) 1107.
- [14] SHEKHTER R. I. *et al.*, *Phys. Rev. Lett.*, **97** (2006) 156801.
- [15] GLAZMAN L. I. and SHEKHTER R. I., *Sov. Phys. JETP*, **67** (1988) 163.
- [16] WINGREEN N. S., JACOBSEN K. W. and WILKINS J. W., *Phys. Rev. Lett.*, **61** (1988) 1396.
- [17] IMAM H. T., PONOMARENKO V. V. and AVERIN D. V., *Phys. Rev. B*, **50** (1994) 18288.
- [18] RAMMER J. and SMITH H., *Rev. Mod. Phys.*, **58** (1986) 323.
- [19] FLENSBERG K., *Phys. Rev. B*, **68** (2003) 205323.
- [20] MITRA A., ALEINER I. and MILLIS A. J., *Phys. Rev. B*, **69** (2004) 245302.
- [21] JAUHO A.-P., WINGREEN N. S. and MEIR Y., *Phys. Rev. B*, **50** (1994) 5528.
- [22] EGGER R. and GOGOLIN A. O., *Phys. Rev. B*, **77** (2008) 113405.
- [23] BOESE D. and SCHOELLER H., *Europhys. Lett.*, **54** (2001) 668.
- [24] KOCH J. and VON OPPEN F., *Phys. Rev. Lett.*, **94** (2005) 206804.
- [25] LETURCQ R. *et al.*, *Nat. Phys.*, **5** (2009) 327.
- [26] CHARLIER J. C., BLASE X. and ROCHE S., *Rev. Mod. Phys.*, **79** (2007) 677.